Clinica Chimica Acta 493 (2019) 79–86

Contents lists available at ScienceDirect

Clinica Chimica Acta

journal homepage: www.elsevier.com/locate/cca

Gene expression changes in cervical squamous cancers following neoadjuvant interventional chemoembolization

Yonghua Chen[a,1], Yuanyuan Hou[a,1], Ying Yang[a,1], Meixia Pan[b], Jing Wang[a], Wenshuang Wang[a], Ying Zuo[a], Jianglin Cong[a], Xiaojie Wang[a], Nan Mu[a], Chenglin Zhang[c], Benjiao Gong[c], Jianqing Hou[a,*], Shaoguang Wang[a,*], Liping Xu[d]

[a] Department of Obstetrics and Gynecology, the Affiliated Yantai Yuhuangding Hospital of Medical College, Qingdao University, Yantai 264000, Shandong, China
[b] Yantai Yuhuangding Hospital LaiShan Division of Medical College, Qingdao University, China
[c] Central Laboratory, the Affiliated Yantai Yuhuangding Hospital of Medical College, Qingdao University, Yantai 264000, Shandong, China
[d] Medical College, Qingdao University, Qingdao 266021, Shandong, China

ARTICLE INFO

Keywords:
Cervical cancer
Chemoembolization
Microarray
AKAP12
CA9

ABSTRACT

Background: The efficacy of therapy for cervical cancer is related to the alteration of multiple molecular events and signaling networks during treatment. The aim of this study was to evaluate gene expression alterations in advanced cervical cancers before- and after-trans-uterine arterial chemoembolization- (TUACE).

Methods: Gene expression patterns in three squamous cell cervical cancers before- and after-TUACE were determined using microarray technique. Changes in AKAP12 and CA9 genes following TUACE were validated by quantitative real-time PCR.

Results: Unsupervised cluster analysis revealed that the after-TUACE samples clustered together, which were separated from the before-TUACE samples. Using a 2-fold threshold, we identified 1131 differentially expressed genes that clearly discriminate after-TUACE tumors from before-TUACE tumors, including 209 up-regulated genes and 922 down-regulated genes. Pathway analysis suggests these genes represent diverse functional categories. Results from real-time PCR confirmed the expression changes detected by microarray.

Conclusions: Gene expression signature significantly changes during TUACE therapy of cervical cancer. Theses alterations provide useful information for the development of novel treatment strategies for cervical cancers on the molecular level.

1. Introduction

As a leading cause of cancer mortality only second to breast cancer in women, cervical cancer (CC) poses a major threat to women's health in the developing countries. Epidemiological studies in the central and Western regions of China indicated that cervical cancer represents a major heath concern for women in rural areas [1]. For decades, radical surgery and radiotherapy have been applied to treat cervical cancer [2], but many cervical cancer cases in developing countries are in late stage or locally advanced cell carcinomas (defined as local tumor size in diameter ≥ 4 cm [3]) with high morbidity and mortality. While radical surgery or radiotherapy are effective for early-stage cervical cancers, late stage cancers often respond poorly to conventional treatment. New therapeutic modalities are urgently needed for the treatment of late stage CC cases.

Trans-uterine arterial chemotherapy (TUAC) with cisplatin followed by trans-uterine artery embolization (UAE) (Trans-uterine arterial chemoembolization , TUACE) has shown relatively high clinical and pathological response rates [4]. There are obvious theoretical advantages of TUACE in CC treatment. The intra-arterial chemotherapy may increase tumor's exposure to high drug concentrations in the local pelvis, which can reach four to 22 times of the concentration by intravenous chemotherapy. TUACE also reduces the systemic drug concentration and hence, better limits the side effect. Combined with embolization, intra-arterial chemotherapy may prolong the effective time of the chemotherapy, simultaneously increases ischemia and necrosis of the tumor tissues, and better control the vaginal hemorrhage [5].

Cisplatin is considered the most effective drug for treatment of cervical cancer. Bleomycin is an antineoplastic antibiotic which inhibits growth factor-induced endothelial cell proliferation, invasion,

* Corresponding authors.
E-mail addresses: houjianqing63@163.com (J. Hou), Shaoguangw@sina.com (S. Wang).
[1] Authors contributed equally to this work.

https://doi.org/10.1016/j.cca.2019.02.012
Received 12 November 2018; Received in revised form 21 January 2019; Accepted 13 February 2019
Available online 14 February 2019
0009-8981/

migration and angiogenesis, and induces endothelial cell apoptosis. The combination of cisplatin and bleomycin is considered an effective neoadjuvant chemotherapeutic regimen, achieving complete response in > 20% of CC cases [6,7]. Microarray technology can be used to determine mRNA expression patterns of numerous genes simultaneously in a single round of hybridization. Studies have thus far focused on differences in gene expression between cervical carcinomas and normal cervical tissues, or between HPV-positive and -negative tissue/cell lines. Clinical studies were also conducted to identify genes predictive of radiosensitivity [8,9]. Herein, we compared global gene expression patterns of cervical tumor samples before and after TUACE. Elucidation of the mechanisms leading to cell death or survival in the TUACE process is required for elimination of tumor resistance and optimization of therapeutic efficacy.

2. Materials and methods

2.1. Patients and tissue sample preparation

The present study included a total of 20 cervical cancer patients treated with TUACE between 2011 and 2015. These patients were registered in Department of Obstetrics and Gynecology, the Affiliated Yantai Yuhuangding Hospital of Medical College, Qingdao University. Three patients (A, B and C) sensitive to TUACE were selected for microarray analysis. A1, B1 and C1 represent samples taken before TUACE, and A2, B2 and C2 were taken after TUACE. The clinicopathological characteristics of these tumor samples are summarized in Table 1.

The inclusion criteria for TUACE subjects were as follows: 1) patients with clinic stage I and II which tumor size in diameter ≥ 4 cm, according to the International Federation of Gynecology and Obstetrics (FIGO); 2) patients whose pathologic examinations showed squamous cell carcinoma of the cervix; 3) patients who did not receive prior hysterectomy, pelvic radiotherapy or concurrent chemo- or radio-therapy.

The response to TUACE was evaluated according to the World Health Organization (WHO) criteria: CR, complete response; PR, partial response; SD, stable disease; PD, progressive disease [10]. CR and PR were considered sensitivity to therapy. Diagnostic criteria of tissue type, grade and pathologic parameter are based on the modified FIGO 2009 staging system. All the patients were staged in accordance with the FIGO criteria.

This project was approved by the Ethics Committee of the Affiliated Yantai Yuhuangding Hospital of Medical College, Qingdao University.

Table 1
Clinicopathologic features of 20 tissue samples used for this study analysis.

Patient No	Patient age (y)	Tumor grade	Tumor stage	Depth of myometrial invasion	Vessel carcinoma embolus
1(A)	36	G3	IB2	< 1/2	No
2(B)	42	G1	IIA2	< 1/2	Yes
3(C)	34	G3	IIA2	> 1/2	Yes
4	36	G3	IB2	< 1/2	No
5	44	G3	IIA2	> 1/2	Yes
6	50	G3	IIA2	> 1/2	No
7	44	G3	IIA2	> 1/2	No
8	66	G2	IIA2	< 1/2	No
9	43	G3	IB2	< 1/2	No
10	38	G3	IB2	> 1/2	Yes
11	59	G3	IIA2	> 1/2	No
12	52	G3	IIA2	< 1/2	No
13	38	G3	IIA2	> 1/2	No
14	42	G1	IB2	< 1/2	No
15	59	G3	IIA2	< 1/2	No
16	49	G3	IIA2	< 1/2	No
17	47	G3	IIA2	> 1/2	Yes
18	35	G2	IIA1	< 1/2	Yes
19	50	G2	IIA2	< 1/2	No
20	54	G2	IIA2	< 1/2	No

All participants signed the informed consent form.

2.2. Biopsy, sample collection, and mRNA extraction

Cervix samples were obtained with biopsy forceps prior to TUACE therapy and at the time of radical hysterectomy after about 3 weeks of TUACE, which were referred to as before-TUACE and after-TUACE, respectively. All biopsy samples were rinsed with ice-cold PBS, and snap frozen with liquid nitrogen before storage at 80 °C for later usage.Total RNA was extracted from the snap-frozen samples using TRIzol reagent (Invitrogen, Carlsbad, California, USA) according to the standard protocol. RNA quality was assessed by measurement of the OD 260/280 ratio using the spectrophotometer ND-1000 (NanoDrop, USA) and only samples with a ratio of ≥1.80 were included. RNA integrity was assessed by denaturing electrophoresis on an agarose formaldehyde gel.

2.3. TUACE treatment

A 5-French plastic catheter was inserted from the right femoral artery using the Seldinger method under local anesthesia. After pelvic angiography was performed, the tip of the catheter was placed in the left intrailiac artery. A 3-French polyethylene catheter was catheterized into the left uterine artery, and 30 mg of Cisplatin and 10 mg of Bleomycin was administered respectively. This was followed by transcatheter arterial embolization using 350 to 560 μm gelatin sponge particles (Alicon, Hangzhou) as described by Wang et al. [11]. Following embolization, elimination of the tumoral bleeding and potency of the arteries not targeted were verified using pelvic angiography. Then 20 mg of Cisplatin and 5 mg of Bleomycin were administered via the left intrailiac artery respectively. The same procedure was performed via the right pelvic artery.

2.4. cDNA microarray

Tissue homogenization, mRNA extraction, and microarray analysis were performed at CapitalBio Corporation, Bejing, China. RNA quality was assessed by measurement of the OD 260/280 ratio using the spectrophotometer ND-1000 (NanoDrop, USA) and only samples with a ratio of ≥1.80 were included. RNA integrity was evaluated by denaturing electrophoresis in agarose formaldehyde gels.

Affymetrix 3′ IVT mRNA GeneChip (PrimeView™ Human Gene Expression Array) and Affymetrix GeneChip Fluidics Station 450 were utilized to determine gene expression. The Affymetrix GeneChip Scanner 3000 was used to analyze the hybridization results. Individual channel data was normalized with locally weighted scatterplot smoothing (LOWESS) algorithm. A gene was regarded as be expressed when the intensity of the hybridization signal was 2.0 fold higher than the background level.

2.5. Microarray data analysis

2.5.1. Unsupervised analysis: cluster analysis

Cluster Software Version 3.0, an unsupervised hierarchical cluster algorithm, was used to group genes and experimental samples tested. Only those genes with > 80% of log-transformed ratio values presenting in all arrays were selected for further study. Median centering and average linkage hierarchical clustering for both genes and arrays was applied. The results were visualized by Java Treeview software.

2.5.2. Supervised analysis: SAM analysis

To detect differentially expressed genes associated with TUACE therapy, we used SAM Version 3.0. The qualified microarray data were imported into a Microsoft Access database and the normalized median of ratio values of the genes were log2 transformed. Genes having *P*-values < 0.05 and showing at least a 2-fold change were selected for parametric Student's test and fold-change analysis.

2.5.3. Pathway analysis

Molecule Annotation System (CB-MAS 3.0) of CapitalBio Corporation is a data-mining and function-annotation solution capable of extracting and analyzing genome-wide relationships between biological molecules from public knowledge bases. In this study, pathway diagrams were generated using CB-MAS 3.0. Genes with > 2.0-fold of change were included for further analyses.

2.6. Quantitative real-time PCR

The expressions of two genes chosen for validation were determined by real-time PCR (Mini Opticon, CFD3120, Bio-Rad, USA) using PCRMasterMix (SYBR Green) (Toyobo Co, Ltd., Japan) following manufacture's protocol. β-actin gene was used as an internal reference. Each reaction was performed in 25 μL volume with final concentration of 1 × SYBR Green mixture, 100 nM primers, 2 μL of 1:5 dilution of the cDNA and RNase-free water. Reactions were carried out under the following cycling conditions: 94 °C for 5 min, 40 cycles of 94 °C for 30 s, 60 °C for 30 s, and 72 °C for 30 s. The results were analyzed using MiniOpticon Real-Time PCR System. The specificity of the amplified products was monitored by its melting curve.

2.7. Statistical methods

The relative expression levels were calculated using the comparative CT method. The mean and SD values are shown in the figures. SPSS Version 22.0 (SPSS Inc., Chicago, IL, USA) was used for statistical analysis. Student's test was applied to analysis of real-time PCR results. A $P < 0.05$ was considered statistically significant.

3. Results

3.1. Hierarchical clustering of tumor samples from before-TUACE group and after-TUACE groups

In the initial analysis of gene expression data, we used an unsupervised two-dimensional hierarchical clustering algorithm to group tumors based on similarities in their gene expression profiles. Cluster analysis revealed two distinct clusters (cluster 1, blue and cluster 2, red) (Fig. 1A and B). As expected, a dendrogram with two distinct arms clearly separates after-TUACE patients from before-TUACE patients. Cluster 1 was composed completely of before-TUACE patients, while Cluster 2 included after-TUACE patients.

3.2. Identification of differentially expressed genes and functional classification

To identify differentially expressed genes that may help to distinguish the after-TUACE tumor from before-TUACE samples, supervised cluster analysis-SAM was utilized. Using a 2-fold threshold, we identified 1131 differentially expressed genes that clearly discriminate the after-TUACE tumors from before-TUACE tumors, including 209 up-regulated genes and 922 down-regulated genes in after-TUACE tumors compared with before-TUACE tumors. These genes represent diverse functional categories, including those for cell cycle, DNA polymerase, p53 signaling pathway, mismatch repair, pyrimidine metabolism, axon guidance, cytokine-cytokine receptor, nucleotide excision repair, ubiquitin mediated proteolysis, checkpoint of mitotic cell cycle, G2/M and G1/S check point of cell cycle and so on (Tables 2, 3 and 4).

3.3. Pathway analysis of differently expressed genes and their functions

To analysis the function connection among the differentially expressed genes and the co-regulated pathways contributing to the distinct biology associated with TUACE, for 1131 differentially expressed genes, we further identified 265 differentially expressed genes using a 5-fold threshold, including 68 up-regulated genes and 197 down-regulated genes in after-TUACE tumors compared with before-TUACE tumors. The 265 differentially expressed genes were analyzed with CB-MAS and the interactions among these genes are shown in Fig. 2, and their biological functions are listed in Tables 2, 3 and 4.

3.4. Verification of differentially expressed genes by qRT-PCR

We selected two differentially expressed genes for validation by qRT-PCR. AKAP12 was up-regulated and CA9 was down-regulated in

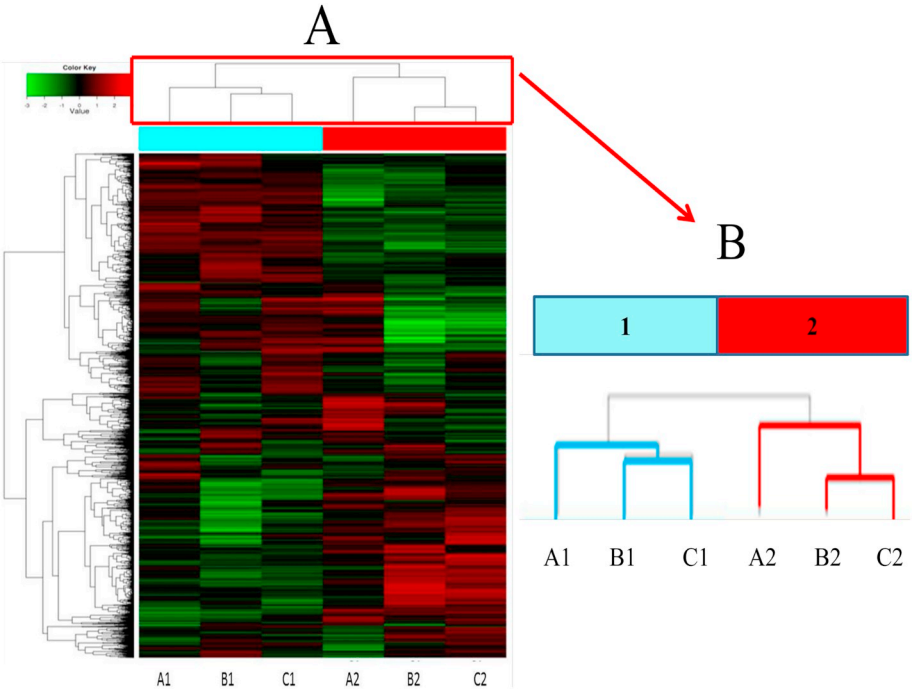

Fig. 1. (A) Hierarchical clustering of gene expression patterns in 6 cervical carcinoma tissue samples. Each row represents a single gene and each column represents a single tissue sample. The expression levels of gene transcripts are represented by different colors: black represents no expression, green represents lower expression and red represents higher expression. Each tissue sample derived from patient is numbered. (B) Tumor samples are grouped based on similarities in their gene expression changes using an unsupervised hierarchical clustering analysis. Cluster analysis revealed two distinct tumor clusters with differential gene expression patterns representing before-TUACE (cluster 1, blue) and after-TUACE (cluster 2, red). (For interpretation of the references to colour in this figure legend, the reader is referred to the web version of this article.)

Table 2
The ten most relevant pathways potentially involved in tumor responses to TUACE in the KEGG analysis.

Pathway	Count	p-Value	q-Value	Gene[a]
DNA polymerase	23	4.71E-37	2.94E-35	LIG1;POLD2;RPA1;POLD1;POLE;RPA2;POLD3;MCM3;RFC3;POLA1;RPA3;PCNA;MCM6;MCM2;MCM7;RFC2;MCM7;RFC5;FEN1;MCM4;RNASEH2A;RFC4;PRIM1;POLE2
Cell cycle	29	4.25E-31	1.32E-29	CCND2;YWHAQ;PRKDC;DBF4;CDC45L;MCM3;ORC5L;CHEK2;ESPL1;PCNA;CDC25C;MCM6;MCM2;MCM7;CDC25A;CCNA2;MAD2L1;MCM7;CHEK1;ORC6L;MCM4;CCNE2;CDC20;CDC2;CDC7;BUB1B;CCNB2;CCNB1;CDKN2A;SMC1B
Mismatch repair	14	1.42E-22	1.77E-21	LIG1;POLD2;RPA1;POLD1;RPA2;POLD3;RFC3;RPA3;MSH6;PCNA;RFC2;RFC5;MSH2;RFC4
Nucleotide excision repair	16	6.40E-21	7.48E-20	ERCC4;LIG1;POLD2;RPA1;POLD1;MNAT1;POLE;RPA2;POLD3;RFC3;RPA3;PCNA;RFC2;RFC5;RFC4;POLE2
Homologous recombination	10	1.82E-13	1.79E-12	POLD2;RPA1;POLD1;SHFM1;RPA2;POLD3;RPA3;RAD51;RAD54L;RAD54B
Pyrimidine metabolism	14	1.31E-12	1.17E-11	POLD2;POLR1A;POLD1;DUT;POLR2H;POLE;POLR1B;POLD3;RRM1;UMPS;POLA1;TK1;PRIM1;POLE2
Purine metabolism	15	1.04E-10	7.21E-10	PDE4A;POLD2;POLR1A;POLD1;AK2;POLR2H;POLE;POLR1B;POLD3;RRM1;POLA1;PKM2;PRIM1;ADSSL1;POLE2
Base excision repair	9	1.16E-10	7.45E-10	LIG1;POLD2;POLD1;POLE;POLD3;PCNA;UNG;FEN1;POLE2
p53 signaling pathway	9	5.10E-08	2.51E-07	CCND2;CHEK2;STEAP3;CHEK1;CCNE2;CDC2;CCNB2;CCNB1;CDKN2A
Glycolysis/Gluconeogenesis	8	3.99E-07	1.73E-06	DLD;TPI1;ALDOA;PGK1;PKM2;ENO1;GPI;ADH7

[a] Count: The number of differentially expressed genes in the pathway; p-Value: Enrichment analysis statistically significant level; q-Value: The value for statistical test of p-value.

after-TUACE tumors compared with before-TUACE tumors (Fig. 3). These genes have > 5-fold changes in expression level based on the qRT-PCR results. The direction of expression change estimated by qRT-PCR are consistent with those estimated from microarray (Table 5). qRT-PCR results confirmed that AKAP12 was significantly up-regulated while CA9 was significantly down-regulated in after-TUACE compared with before-TUACE.

4. Discussion

Despite the recent advances in surgery and radiotherapy, the therapeutic efficacy for patients with locally advanced cervical cancer is poor. Many patients have subsequent local recurrence and metastasis, and these patients' long survival rates have not been much improved over the past decade. New therapeutic approaches are required for treating the advanced cervical cancer. In recent years, the neoadjuvant chemotherapy (NACT) is increasingly applied to treat cervical cancers [12,13].

Chemotherapy prior to surgery can help to prepare tumors unfit for surgery to be operable. Moreover, radiotherapy tends to injure adjacent organs, more and more patients choose NACT plus surgery rather than radiotherapy. At present, there are two approaches for NACT, intravenous systematic chemotherapy or intra-arterial interventional chemotherapy. Intravenous administration is relatively economic and simple, but can cause more side effects. Intra-arterial interventional chemotherapy, also known as uterine arterial chemoembolization, can increase the drug concentration at the tumor level and reduce toxicity. There is a debate on the efficacy of TUACE. Yamakawa et al. [14] found that neoadjuvant intra-arterial chemotherapy is able to effectively eliminate the pathologic risk factors in the pelvic cavity, to improve the operability in patients with stage IIIB cervical cancer that is often considered inoperable, and to improve the prognosis of patients with locally advanced cervical cancers. Multiple reports have confirmed the significance of arterial interventional chemoembolization for uterine cancer therapy [15]. While Tian et al. [16] indicated that the use of TUACE before radical radiotherapy would significantly decrease long-time survival. The discrepancy of above mentioned studies could be due to the treatment regimen after intra-arterial interventional therapy: in the former study it was radical surgery whereas in the latter it was radiotherapy. A meta-analysis of neoadjuvant chemotherapy followed by radical hysterectomy showed an absolute improvement of 14% in the five-year survival [17]. Therefore, the multi-modality therapy including a combination of TUACE and the following radical surgery may be the optional treatment for CC.

Combined with embolization, intra-arterial interventional therapy does not only involves uterine arterial infusion of drugs, but also blocks the blood supply, which leads to tumor anoxia, hypoxia, and ultimately, cell apoptosis and ischemic tissue necrosis [16]. However, accumulating evidence indicated that severe tumor hypoxia may be associated with resistance to chemoradiotherapy [18,19] and may promote metastatic spread of locally advanced carcinoma of the uterine cervix [16,20]. From a radiotherapy perspective, hypoxia of tumor cells would induce radiation resistance that may contribute to the negative effects of long-term radiotherapy [18]. The regime of interventional therapy plus radical operation could resect all the potentially resistance cells.

Albeit the theoretical advantage of intra-arterial interventional therapy, due to tumor molecular heterogeneity, there are still some patients being resistant to the therapy. Biomarkers capable of predicting the treatment outcomes of TUACE would be very useful for the management of late stage CC cases. Interestingly, the microarray-based platform has been used to compare gene expression profiles of cervical cancers and normal tissues, or before and after chemotherapy, but the difference between before- and after-intra-uterine-artery interventional therapy has not been explored in cervical cancer. Our microarray analysis demonstrated that 1131 genes displayed significant differences in their expression between the two groups of before- and after-

Table 3
The ten most relevant pathways in the GenMAPP analysis.

Pathway	Count	p-Value	q-Value	Gene[a]
GO_Samples–Biological process–DNA replication	40	6.71E-47	1.25E-44	GMNN;LIG1;POLD2;RPA1;POLD1;DUT;POLE;RPA2;-CDC45L;NFIA;POLD3;WRNIP1;MCM3;ORC5L;RR-M1;RFC3;POLA1;RPA3;MSH6;RAD51;CDT1;PCNA;P-OLQ;MCM6;MCM8;MCM2;MCM7;RFC2;CHAF1A;M-CM7;RFC5;MSH2;FEN1;ORC6L;MCM4;NCOA6;RNA-SEH2A;RFC4;CDC7;POLE2;GINS2
Contributed–cellular_process–Hs_DNA_replication_Reactome	28	1.10E-45	1.03E-43	GMNN;POLD2;RPA1;POLD1;DBF4;POLE;RPA2;CD-C45L;POLD3;MCM3;ORC5L;RFC3;POLA1;RPA3;CD-T1;PCNA;MCM6;MCM2;MCM7;RFC2;MCM10;MC-M7;RFC5;ORC6L;MCM4;RFC4;CDC7;PRIM1;POLE2
GO_Samples–Biological process–M phase	34	5.83E-34	2.72E-32	DDX11;MSH6;RAD51;CCNF;SMC2;ESPL1;KIF15;RA-D54L;CDC25C;CDC25A;SMC4;CCNA2;MAD2L1;NC-APD2;NDC80;UBE2C;CHEK1;RAD54B;CDC20;TPX2;-AURKA;SPAG5;PRC1;KIF2C;KIF23;CDC2;BUB1B;AS-PM;NEK2;CCNB2;CCNB1;TTK;SMC1B;SYCP2
Contributed–cellular_process–Hs_Cell_cycle_KEGG	27	6.30E-32	2.36E-30	CCND2;PRKDC;DBF4;CDC45L;MCM3;ORC5L;CHE-K2;ESPL1;PCNA;CDC25C;MCM6;MCM2;MCM7;CD-C25A;CCNA2;MAD2L1;MCM7;CHEK1;ORC6L;MC-M4;CCNE2;CDC20;CDC2;CDC7;BUB1B;CCNB2;CCN-B1;CDKN2A
GO_Samples–Biological process–response to DNA damage stimulus	33	2.38E-29	6.36E-28	BTG2;ERCC4;RAD1;LIG1;RPA1;DDX11;POLD1;PRK-DC;MNAT1;POLE;POLD3;WRNIP1;CHEK2;FANCL;R-PA3;NUDT1;RAD51AP1;MSH6;RAD51;ATRX;RA-D54L;PCNA;POLQ;FANCE;CHAF1A;UNG;RFC5;MS-H2;FEN1;CHEK1;RAD54B;NCOA6;POLE2
GO_Samples–Biological process–response to endogenous stimulus	33	2.03E-28	4.76E-27	BTG2;ERCC4;RAD1;LIG1;RPA1;DDX11;POLD1;PRK-DC;MNAT1;POLE;POLD3;WRNIP1;CHEK2;FANCL;R-PA3;NUDT1;RAD51AP1;MSH6;RAD51;ATRX;RA-D54L;PCNA;POLQ;FANCE;CHAF1A;UNG;RFC5;MS-H2;FEN1;CHEK1;RAD54B;NCOA6;POLE2
GO_Samples–Biological process–DNA repair	31	3.61E-28	7.50E-27	BTG2;ERCC4;RAD1;LIG1;RPA1;DDX11;POLD1;PRK-DC;MNAT1;POLE;POLD3;WRNIP1;FANCL;RPA3;NU-DT1;RAD51AP1;MSH6;RAD51;ATRX;RAD54L;PCN-A;POLQ;FANCE;CHAF1A;UNG;RFC5;MSH2;FEN1;R-AD54B;NCOA6;POLE2
GO_Samples–Biological process–M phase of mitotic cell cycle	27	1.34E-27	2.50E-26	DDX11;CCNF;SMC2;ESPL1;KIF15;CDC25C;CDC25A;-SMC4;CCNA2;MAD2L1;NCAPD2;NDC80;UBE2C;CD-C20;TPX2;AURKA;SPAG5;PRC1;KIF2C;KIF23;CDC2;-BUB1B;ASPM;NEK2;CCNB2;CCNB1;TTK
Contributed–cellular_process–Hs_Cell_Cycle-G1_to_S_control_Reactome	22	3.99E-27	6.79E-26	CCND2;RPA1;MNAT1;POLE;RPA2;CDC45L;MCM3;-ORC5L;RPA3;CREB3L4;PCNA;MCM6;MCM2;MCM7;-CDC25A;MCM7;ORC6L;MCM4;CCNE2;PRIM1;CCN-B1;POLE2;CDKN2A
GO_Samples–Biological process–cytokinesis	25	7.77E-26	1.16E-24	CCND2;LIG1;CABLES2;CKS2;CCNF;ESPL1;CDC25C;-CDC25A;CCNA2;UBE2C;CCNE2;CDC20;CKS1B;CDC-A8;SPAG5;CDCA5;PRC1;KIF23;CDC2;CDC7;NEK2;C-CNB2;CDCA7;CCNB1;SYCP2

[a] Count: The number of differentially expressed genes in the pathway; p-Value: Enrichment analysis statistically significant level; q-Value: The value for statistical test of p-value.

Table 4
The ten most relevant pathways in the BioCarta analysis.

Pathway	Count	p-Value	q-Value	Gene
CDK regulation of DNA replication	8	1.52E-16	1.58E-15	MCM3;ORC5L;CDT1;MCM6;MCM2;MCM7;MCM7;ORC6L;MCM4
Sonic Hedgehog (SHH) receptor Cell cycle regulation	6	9.60E-12	7.80E-11	XPO1;MNAT1;CDC25C;CDC25A;CDC2;CCNB1
Cell cycle: G2/M checkpoint	8	1.03E-11	8.06E-11	YWHAQ;PRKDC;CHEK2;CDC25C;CDC25A;CHEK1;CDC2;CCNB1
Role of BRCA1, BRCA2 and ATR in cancer susceptibility	6	4.73E-08	2.39E-07	RAD1;CHEK2;RAD51;FANCE;FANCD2;CHEK1
cdc25 and chk1 regulatory pathway in response to DNA damage	4	6.21E-08	2.98E-07	CDC25C;CDC25A;CHEK1;CDC2
Activation of Src by Protein-tyrosine phosphatase alpha	4	4.27E-07	1.82E-06	CDC25C;CDC25A;CDC2;CCNB1
RB tumor suppressor/checkpoint signaling in response to DNA damage	4	1.51E-06	5.55E-06	CDC25C;CDC25A;CHEK1;CDC2
Role of Ran in mitotic spindle regulation	4	2.50E-06	8.82E-06	RANBP1;KIF15;TPX2;AURKA
Cyclins and cell cycle regulation	5	3.79E-06	1.26E-05	CCND2;CDC25A;CDC2;CCNB1;CDKN2A
Stathmin and breast cancer resistance to antimicrotubule agents	4	3.89E-06	1.28E-05	MAPK13;STMN1;CDC2;CCNB1

Count: The number of differentially expressed genes in the pathway; p-Value: Enrichment analysis statistically significant level; q-Value: The value for statistical test of p-value.

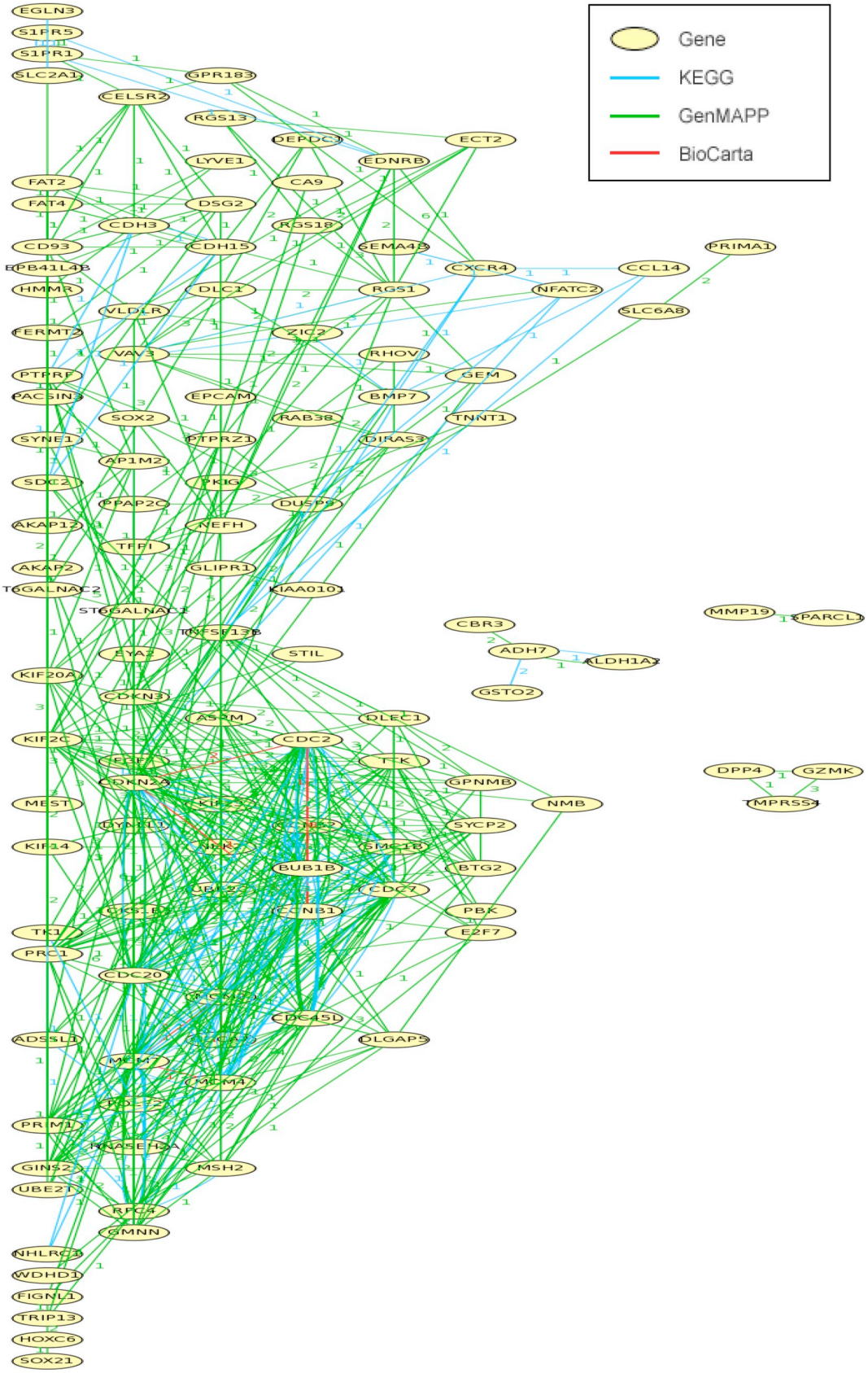

Fig. 2. Pathway analysis of differentially expressed genes identified in after-TUACE compared to before-TUACE.

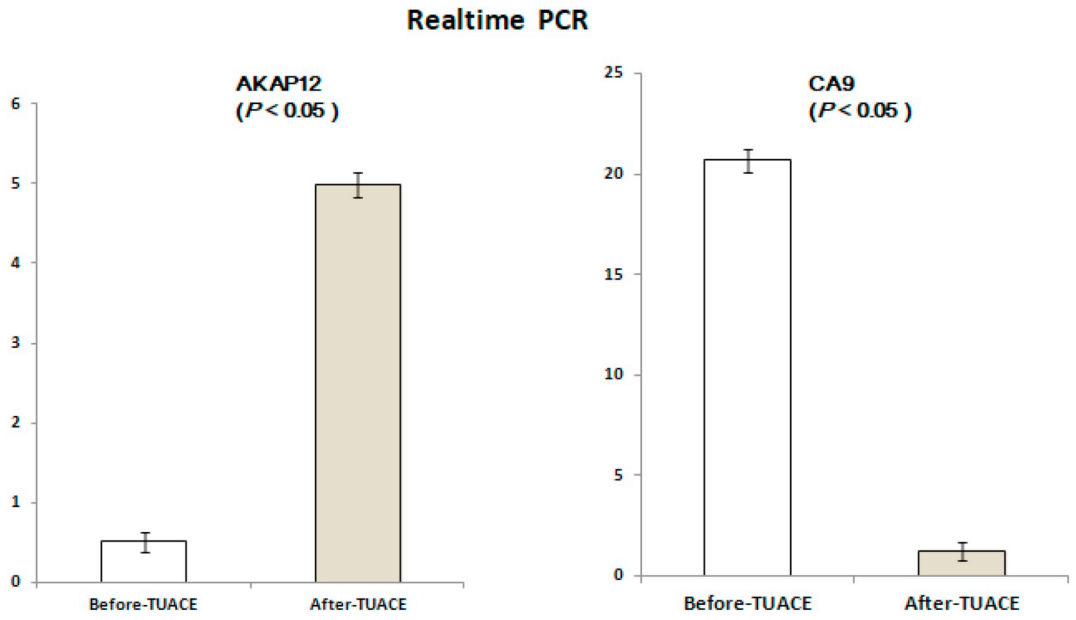

Fig. 3. Real-time PCR analysis of 2 selected genes differentially expressed between before-TUACE and after-TUACE. qRT-PCR results confirmed that AKAP12 was significantly up-regulated while CA9 was significantly down-regulated in after-TUACE samples compared with that in before-TUACE samples.

Table 5
Microarray expression analysis and qRT-PCR validation of two differentially expressed genes between before- and after-TUACE.

Gene	Microarray	Real-time PCR	Trend of changes
AKAP12	10.93	9.76	Consistent
CA9	0.054	0.06	Consistent

interventional treatment. Functional analysis indicated that these genes are responsible for a diverse set of cell functions, supporting that therapy leads to alteration of multiple molecular events and signaling networks.

The A-kinase anchor protein 12 (AKAP12, also known as Gravin) was one of the most up-regulated genes after interventional treatment in this study. Studies from other groups have demonstrated that AKAP12 functions as a tumor suppressor in several human primary cancers, as its decreased expression in cancer cells is directly associated with an increased cancer cell invasion and metastasis [21]. Low expression of AKAP12 was detected in various solid tumor types, including gastric, lung, ovarian and pancreatic cancers. Moreover, promoter hypermethylation was implicated in the loss of AKAP12 expression in cancer cells [22–27]. Its up-regulation by treatments may suppress oncogenic growth and tumor metastasis [28]. AKAP12 expression is also affected by other tumor suppressor gene products that antagonize the oncogenic transformation. For example, AKAP12 is up-regulated by re-expression of the p53 tumor suppressor in cancer cells [29]. Moreover, some studies reveals that AKAP12 could down-regulate the level of hypoxia-inducible factor-1α (HIF-1α) protein by enhancing the interaction of HIF-1α with pVHL (von Hippel-Lindau tumor suppressor protein) and PHD2 (prolyl hydroxylase 2) during blood–retinal barrier formation [30].

Carbonic anhydrase 9 (CA9) was one of the most down-regulated genes after interventional treatment. CA9 is a metalloprotein that catalyzes the reversible hydration of carbon dioxide. It is constitutively up-regulated in several types of cancers, and plays a key role in tumor progression and metastasis [31]. High expression of CA9 is generally associated with poor prognosis and is related to a decreased disease-free interval [31]. The promoter of the *CA9* gene contains an HRE (hypoxia responsive element) that is located immediately upstream of the transcription start site at position −3/−10. HIF-1α binds to the HRE and induces transcription of the *CA9* gene in response to hypoxia [31]. Uterine arterial chemoembolization may lead to a decreased oxygen supply as well as an increased exposure of the tumor and surrounding tissues to high drug concentrations. Hypoxia can induce tumor resistance to chemotherapy or radiation therapy [19]. At the molecular level, HIF-1 is up-regulated in response to oxygen deprivation, binds to the HRE, and controls the transcriptional activity of numerous downstream genes, such as CA9, which has emerged as a promising marker for cell hypoxia. Since AKAP12 is reported to regulate HIF-1α expression, we can postulate that there might be an AKAP12-Hypoxia-CA9 regulatory network during uterine arterial chemoembolization. Further studies are required to prove the existence and significance of this network in TUACE treatment.

Conflict of interest statement

The authors declare that there are no conflicts of interest.

Acknowledgments

This study was supported by Yantai Science and Technology Development Project (NO:2013WS206).

References

[1] B. Song, C. Ding, W. Chen, et al., Incidence and mortality of cervical cancer in China, 2013, Chin. J. Cancer Res. 29 (2017) 471–476.
[2] Chemoradiotherapy for Cervical Cancer Meta-Analysis Collaboration, Reducing uncertainties about the effects of chemoradiotherapy for cervical cancer: a systematic review and meta-analysis of individual patient data from 18 randomized trials, J. Clin. Oncol. 26 (2008) 5802–5812.
[3] M. Hirakawa, Y. Nagai, M. Inamine, et al., Predictive factor of distant recurrence in locally advanced squamous cell carcinoma of the cervix treated with concurrent chemoradiotherapy, Gynecol. Oncol. 108 (1) (2008) 126–129.
[4] H. Tsubamoto, H. Maeda, R. Kanazawa, et al., Phase II trial on neoadjuvant intravenous and trans-uterine arterial chemotherapy for locally advanced bulky cervical adenocarcinoma, Gynecol. Oncol. 129 (2013) 129–134.
[5] Lei Yu, Guo-sheng Tan, Xian-hong Xiang, et al., Comparison of uterine artery chemoembolization and internal iliacarterial infusion chemotherapy for the combining treatment for women with locally advanced cervical cancer, Chin. J. Cancer

28 (2009) 402–407.
[6] Uma Singh, Neetu Ahirwar, Anju Kumari Rani, et al., The efficacy and safety of neoadjuvant chemotherapy in treatment of locally advanced carcinoma cervix, J. Obstet. Gynaecol. India 63 (2013) 273–278.
[7] A.H. Klopp, P.J. Eifel, Chemoradiotherapy for cervical cancer in 2010, Curr. Oncol. Rep. 13 (2011) 77–85.
[8] K. Zempolich, C. Fuhrman, B. Milash, et al., Changes in gene expression induced by chemoradiation in advanced cervical carcinoma: a microarray study of RTOG C-0128, Gynecol. Oncol. 109 (2008) 275–279.
[9] I. Eke, A.Y. Makinde, M.J. Aryankalayil, et al., Comprehensive molecular tumor profiling in radiation oncology: how it could be used for precision medicine, Cancer Lett. 382 (2016) 118–126.
[10] T. Hu, S. Li, Y. Chen, et al., Matched-case comparison of neoadjuvant chemotherapy in patients with FIGO stage IB1-IIB cervical cancer to establish selection criteria, Eur. J. Cancer 48 (2012) 2353–2360.
[11] S. Wang, X. Meng, Y. Dong, The evaluation of uterine artery embolization as a nonsurgical treatment option for adenomyosis, Int. J. Gynaecol. Obstet. 133 (2016) 202–205.
[12] J.E. Sardi, M.A. Boixadera, J.J. Sardi, Neoadjuvant chemotherapy in cervical cancer: a new trend, Curr. Opin. Obstet. Gynecol. 17 (2005) 43–47.
[13] S. Li, T. Hu, Y.L. Chen, Adjuvant chemotherapy, a valuable alternative option in selected patients with cervical cancer, PLoS ONE 8 (9) (2013) e73837.
[14] Y. Yamakawa, M. Fujimura, T. Hidaka, et al., Neoadjuvant intraarterial infusion chemotherapy in patients with stage IB2-IIIB cervical cancer, Gynecol. Oncol. 77 (2000) 264–270.
[15] Y. Kaneyasu, N. Nagai, Y. Nagata, et al., Intra-arterial infusion chemotherapy using cisplatin with radiotherapy for stage III squamous cell carcinoma of the cervix, Int. J. Radiat. Oncol. Biol. Phys. 75 (2009) 369–377.
[16] Z.Z. Tian, S. Li, Y. Wang, et al., Investigation of uterine arterial chemoembolization and uterine arterial infusion chemotherapy for advanced cervical cancer before radical radiotherapy: a long-term follow-up study, Arch. Gynecol. Obstet. 290 (2014) 155–162.
[17] Neoadjuvant Chemotherapy for Cervical Cancer Meta-Analysis Collaboration (NACCCMA) Collaboration, Neoadjuvant chemotherapy for locally advanced cervix cancer, Cochrane Database Syst. Rev. (2004) CD001774.
[18] P. Vaupel, O. Thews, M. Hoeckel, Treatment resistance of solid tumors: role of hypoxia and anemia, Med. Oncol. 18 (2001) 243–259.
[19] J. Markowska, J.P. Grabowski, K. Tomaszewska, et al., Significance of hypoxia in uterine cervical cancer. Multicentre study, Eur. J. Gynaecol. Oncol. 28 (2007) 386–388.
[20] J. Bussink, J.H. Kaanders, A.J. van der Kogel, Tumor hypoxia at the micro-regional level: clinical relevance and predictive value of exogenous and endogenous hypoxic cell markers, Radiother. Oncol. 67 (2003) 3–15.
[21] I.H. Gelman, L. Gao, SSeCKS/Gravin/AKAP12 metastasis suppressor inhibits podosome formation via RhoA- and Cdc42-dependent pathways, Mol. Cancer Res. 4 (2006) 151–158.
[22] M.C. Choi, H.S. Jong, T.Y. Kim, et al., AKAP12/Gravin is inactivated by epigenetic mechanism in human gastric carcinoma and shows growth suppressor activity, Oncogene 23 (2004) 7095–7103.
[23] U. Jo, Y.M. Whang, H.K. Kim, Y.H. Kim, AKAP12alpha is associated with promoter methylation in lung cancer, Cancer Res. Treat. 38 (2006) 144–151.
[24] V.F. Bonazzi, D. Irwin, N.K. Hayward, Identification of candidate tumor suppressor genes inactivated by promoter methylation in melanoma, Genes Chromosom. Cancer 48 (2009) 10–21.
[25] W.A. Mardin, K.O. Petrov, A. Enns, et al., SERPINB5 and AKAP12- expression and promoter methylation of metastasis suppressor genes in pancreatic ductal adenocarcinoma, BMC Cancer 10 (2010) 549.
[26] M. Hayashi, S. Nomoto, M. Kanda, et al., Identification of the A-kinase anchor protein 12 (AKAP12) gene as a candidate tumor suppressor of hepatocellular carcinoma, J. Surg. Oncol. 105 (2012) 381–386.
[27] B. Goeppert, C.R. Schmidt, L. Geiselhart, et al., Differential expression of the tumor suppressor A-kinase anchor protein 12 in human diffuse and pilocytic astrocytomas is regulated by promoter methylation, J. Neuropathol. Exp. Neurol. 72 (2013) 933–941.
[28] Nicholas W. Bateman, Elizabeth Jaworski, Wei Ao, et al., Elevated AKAP12 in paclitaxel-resistant serous ovarian cancer cells is prognostic and predictive of poor survival in patients, J. Proteome Res. 14 (2015) 1900–1910.
[29] S.S. Daoud, P.J. Munson, W. Reinhold, et al., Impact of p53 knockout and topotecan treatment on gene expression profiles in human colon carcinoma cells: a pharmacogenomic study, Cancer Res. 63 (2003) 2782–2793.
[30] Y.K. Choi, J.H. Kim, W.J. Kim, et al., AKAP12 regulates human blood-retinal barrier formation by downregulation of hypoxia-inducible factor-1alpha, J. Neurosci. 27 (2007) 4472–4481.
[31] N.K. Tafreshi, M.C. Lloyd, M.M. Bui, et al., Carbonic anhydrase IX as an imaging and therapeutic target for tumors and metastases, Subcell. Biochem. 75 (2014) 221–254.